# Global map of the gravity anomaly corrected for complete effects of the topography, and of density contrasts of global ocean, ice, and sediments

R. Tenzer, Hamayun
Delft Institute of Earth Observation and Space Systems (DEOS),
Delft University of Technology[1]

P. Vajda
Geophysical Institute of the Slovak Academy of Sciences[2]

A b s t r a c t :  We compile a global map of the sediments, ice and bathymetry stripped topographically corrected gravity anomalies using the spherical harmonic representation of the gravity field. The complete topographic effect to the gravity anomaly comprises the direct topographic effect and the secondary indirect topographic effect. Gravitational effects of the density contrasts of three considered global structural crustal elements – oceans, sediments, and ice – are removed (stripped) from the topographically corrected gravity anomaly. The complete effects of these density contrasts also consist of the direct and the secondary indirect effects. In this study, we model globally the complete effects of the topography and of density contrasts (relative to average crustal density) of major anomalous geological structures inside the Earth's crust due to ocean, ice, and (marine and continental) sediments. The gravity anomalies are computed from the coefficients of a global geopotential model (GGM) with a spectral resolution complete to degree 180. The same spectral resolution is used to compute the complete effects to the gravity anomaly due to the topography and bathymetry. The coefficients of a global elevation model (GEM) are used to compute the complete topographical effect, adopting the average crustal density 2670 kg/m$^3$. The coefficients of a global bathymetric (ocean-depth) model (GBM) are used to compute the complete bathymetric (ocean density contrast) effect, adopting the mean ocean saltwater density 1030 kg/m$^3$. The coefficients of a global ice thickness model (GITM) generated from the 2×2 arc-deg geographical grid of ice thickness data are used to compute the complete ice density contrast effect with a spectral resolution complete to degree 90, adopting the mean ice density 913 kg/m$^3$. Finally, the global data of sediment thickness and density with the 2×2 arc-deg geographical resolution are used to compute the complete sediment mass density contrast effect.

[1] Kluyverweg 1, 2629 HS Delft, The Netherlands; e-mail: r.tenzer@tudelft.nl
[2] Dúbravská cesta 9, 845 28 Bratislava, Slovak Republic; e-mail: Peter.Vajda@savba.sk

## 1. Introduction

While the gravity disturbance is defined as a vertical derivative of the disturbing potential, the formulation of the gravity anomaly is based on the fundamental gravimetric equation. The second term of the fundamental gravimetric equation represents the distinction between the gravity anomaly and the gravity disturbance, which has also implications to the application of the topographic and stripping corrections (e.g., *Vajda et al., 2007*). As a consequence, the application of the topographic and stripping corrections to the gravity anomaly gives origin to the secondary indirect effects. The motivation for defining and using gravity anomalies is historical. When geodetic heights (heights above a reference ellipsoid) were not readily observable, the normal gravity could not have been evaluated at the observation point (typically located at the Earth's surface), only at a vertically displaced (by the height anomaly) point respective to the observation point (thus typically on the telluroid). This had lead to formulating the gravity anomalies.

The gravity anomalies have been used in geodesy for instance in gravimetric geoid modelling. The geoid computation, as a solution to the boundary-value problem, the geoid being the boundary, requires (due to harmonicity) that no masses be present above the boundary. Consequently, the effect of topographic (and atmospheric) masses above the geoid must be removed from the gravity anomalies that enter the geoid computation (under the Stokes scheme). When the gravity anomaly is used, the topographic correction (the removal of the effect of topographic masses above the geoid) consists of two terms: the direct topographical effect and the secondary indirect topographic effect; cf. *Vaníček et al. (2004)*. The gravimetric geoid can be determined also from the gravity disturbances utilizing the Hotine integral. The topographic correction to the gravity disturbance then consists only of the direct topographical effect. Obviously, the application of stripping corrections to the gravity anomaly/disturbance for modelling the density contrasts within the Earth's crust bellow the geoid surface is not needed in geodetic applications.

In geophysics, the major task is to solve the inverse problem of gravimetry, that is, to find the sought anomalous masses. The problem is formulated typically in terms of the attraction, although other parameters of gravity field derived from the disturbing potential may be used as well (e.g., *Vajda et al., 2006)*. The masses of the Earth, and equivalently their attraction, are decomposed into reference and anomalous parts, e.g., into reference and anomalous topographic masses, and into reference and anomalous masses inside the reference ellipsoid. The fact that the reference ellipsoid, not the geoid, is the dividing surface delineating the ellipsoid-referenced topographic masses from below for geophysical purposes is implied (in the decomposition) by the normal gravity being generated by the normal ellipsoid (the geocentric biaxial properly oriented equipotential reference ellipsoid). The reference ellipsoidal masses (the model normal density distribution) are chosen such that they generate the well-known normal gravity (e.g., *Vajda et al., 2006)*. The reference topographic masses generate attraction of the topography that is removed from gravity data in terms of the topographic correction. The formulation of the inverse problem in terms of attraction leads to an implicit use of the gravity disturbance *(Vajda et al., 2006 and 2008)*.

Despite the gravity anomalies are not well suited for the gravimetric inversion (due to additional computations of the secondary indirect effects; cf., *Vajda et al., 2007)*, their use for the gravimetric inversion and interpretation is still optional due to the fact that until now the gravity anomalies are the most commonly available gravity data type. In *Tenzer et al. (2008)*, we modelled globally the secondary indirect effects of the topography and of density contrasts due to ocean, ice, and sediments. In this study, we compute the corresponding complete effects and apply them to the gravity anomalies in order to compile a global map of the sediment, ice and bathymetry stripped topographically corrected gravity anomalies. Due to a low resolution and expected accuracy of global modelling the complete effects in this study, the gravitational effect of continental glaciers (expect for Greenland and Antarctica) and water bodies is not considered. Moreover, the geoid-referenced complete effects are computed instead of more rigorous ellipsoid-referenced complete effects.

## 2. Global complete topographic and ice, sediment, and bathymetric stripping corrections to the gravity anomaly

The $5 \times 5$ arc-min global elevation data from ETOPO5 (provided by the NOAA's National Geophysical Data Centre) were used to generate the GEM coefficients. These coefficients were then used to compute the complete topographic effect with a spectral resolution complete to degree and order 180. The mean topographic (average crustal) density 2670 kg/m$^3$ was adopted. We note that the expressions for modelling the topography-generated gravitational potential and attraction from the GEM coefficients can be found for instance in (*Vaníček et al., 1995; Novák and Grafarend, 2006*).

The $5 \times 5$ arc-min global bathymetry data from ETOPO5 were used to generate the GBM coefficients from which the complete bathymetric effect was computed with a spectral resolution complete to degree and order 180. The mean value of the ocean density contrast –1640 kg/m$^3$ (i.e., the difference between the mean ocean saltwater density 1030 kg/m$^3$ and the average crustal density 2670 kg/m$^3$ was adopted.

The discrete data of ice thickness with the $2 \times 2$ arc-deg geographical resolution from the global crustal model CRUST 2.0 (`http://mahi.ucsd.edu /Gabi/rem.dir/crust/crust2.html`) were used to generate the GITM coefficients. The GITM and GEM coefficients were used to compute the complete ice density contrast effect with a spectral resolution complete to degree and order 90. The mean value of the ice density contrast –1757 kg/m$^3$ (i.e., the difference between the mean ice density 913 kg/m$^3$ and the average crustal density 2670 kg/m$^3$) was adopted.

The $2 \times 2$ arc-deg global data of soft and hard sediment thickness and density from the CRUST 2.0 were used to compute the complete sediment density contrast effect. The corresponding values of the sediment density contrasts are defined with respect to the average crustal density 2670 kg/m$^3$.

The complete corrections to the gravity anomaly due to the topography, bathymetry, ice density contrast, and sediment density contrast, all being computed at the $1 \times 1$ arc-deg geographical grid of points at the Earth's surface, are shown in Figs. 1 through 4, and statistics are summarized in Table 1. Statistics of the corresponding direct and secondary indirect effects are summarized in Tables 2 and 3. The complete topographic correction

to the gravity anomaly ranges from –377.7 to 258.8 mGal (see Fig. 1). In mountainous regions, negative values of the complete topographic correction reach several hundred miligals due to a presence of large negative values of the direct topographic effect. In oceanic areas and over flat regions, the direct topographic effect is much smaller while the long-wavelength secondary indirect effect is still present. Hence, the complete topographic correction is mostly positive and almost equal to the secondary indirect effect. The complete bathymetric correction to the gravity anomaly ranges from –643.6 to –32.2 mGal (see Fig. 2). The absolute maxima are located in continental areas with a main contribution from the long-wavelength secondary indirect bathymetric effect. Over oceanic areas, the complete bathymetric correction is much smaller due to the fact that a large contribution of the direct bathymetric effect is significantly reduced when combined with the secondary indirect bathymetric effect. In areas covered by the polar ice sheet, the complete ice density contrast correction to the gravity anomaly ranges from –53.0 to 199.1 mGal (see Fig. 3). The complete sediment density contrast correction to the gravity anomaly ranges from –92.5 to 33.2 mGal (see Fig. 4). The maxima are mainly located over continental shelves and the Caspian Sea region. The minima are in areas of the open ocean.

The errors of modelling the topography-generated gravitational field

Table 1. Statistics of the complete corrections to the gravity anomaly due to the topography, bathymetry, ice density contrast, and sediment density contrast

| Complete correction to the gravity anomaly | Min (mGal) | Max (mGal) | Mean (mGal) | STD (mGal) |
|---|---|---|---|---|
| topographic | -377.7 | 258.8 | 104.5 | 94.5 |
| bathymetric | -643.6 | -32.2 | -375.6 | 101.9 |
| ice density contrast | -53.0 | 199.1 | -1.4 | 36.7 |
| sediment density contrast | -92.5 | 33.2 | -35.2 | 15.9 |

of the average crustal density are expected to be small, provided that the GEM coefficients are generated very accurately from existing high-resolution and high-accuracy digital terrain models. The currently available high-resolution bathymetric data combined with the oceanographic models of salinity and temperature allow an accurate modelling of the gravitational field generated by the ocean density contrast. In this study, we adopted

Table 2. Statistics of the direct effects to the gravity anomaly due to the topography, bathymetry, ice density contrast, and sediment density contrast

| Direct effect | Min (mGal) | Max (mGal) | Mean (mGal) | STD (mGal) |
|---|---|---|---|---|
| topographical | -622.9 | 72.0 | -15.4 | 92.2 |
| bathymetric | 128.7 | 752.5 | 326.8 | 161.2 |
| ice density contrast | 2.5 | 300.3 | 21.9 | 56.2 |
| sediment density contrast | -6.9 | 121.7 | 35.3 | 22.1 |

Table 3. Statistics of the secondary indirect effects to the gravity anomaly due to the topography, bathymetry, ice density contrast, and sediment density contrast

| Secondary indirect effect | Min (mGal) | Max (mGal) | Mean (mGal) | STD (mGal) |
|---|---|---|---|---|
| topographical | 74.2 | 278.4 | 119.8 | 36.7 |
| bathymetric | -895.6 | -514.5 | -702.4 | 100.4 |
| ice density contrast | -109.8 | -10.0 | -23.3 | 23.0 |
| sediment density contrast | -98.2 | -50.6 | -70.4 | 12.3 |

the mean value of the ocean saltwater density. Since the anomalous ocean saltwater density variations with respect to the mean value 1030 kg/m$^3$ are within the interval from –10 to 20 kg/m$^3$, the relative errors of modelling the gravitational field generated by the ocean density contrast can reach 2% at the most. The corresponding errors of the complete bathymetric correction up to a few dozens of miligals are expected at the computation points situated over oceanic areas. Over continental areas, these errors decrease significantly. For a more accurate computation, the existing oceanographic models of salinity, temperature and pressure (depth) should be facilitated to determine more realistically the ocean saltwater density distribution. According to *Millero and Poisson (1981)*, the equation of state of seawater now allows the calculation of density to a fractional accuracy of 0.03 kg/m$^3$. Whereas large errors of modelling the gravitational field generated by the ice density contrast are expected in polar areas due to inaccuracies within the currently available global ice sheet thickness data, errors due to small ice density variations are much smaller. Large errors of modeling the gravitational field generated by the sediment density contrast are expected over
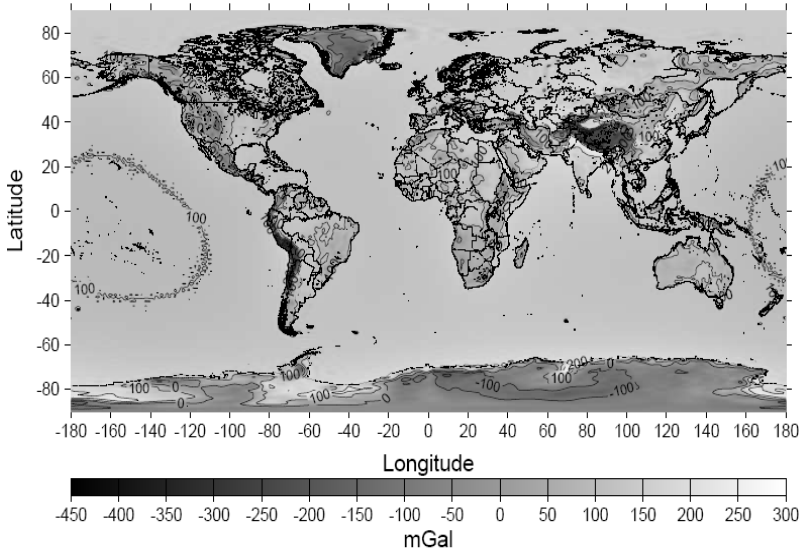
Fig. 1. The global complete topographic correction to the gravity anomaly at the Earth's surface computed with a spectral resolution complete to degree and order 180 of the GEM coefficients. The average crustal density 2670 kg/m$^3$ was adopted.

areas of the largest sediment density variations within the upper Earth's crust. Another source of errors is due to unmodeled crustal density variations such as a different density of the oceanic and continental crust.

## 3. Global map of the sediment, ice, and bathymetry stripped topographically corrected gravity anomalies

The GGM coefficients taken from the EGM-96 *(Lemoine et al., 1998)* complete to degree and order 180 were used to compute the gravity anomalies. As stated in the previous section, large errors are expected in modelling the stripping corrections. Therefore, the choice of more recent global geopotential models for computing the Earth's gravity field was not considered essential. The computation was realized at the $1 \times 1$ arc-deg geographical grid of points at the Earth's surface. The expressions for computing the
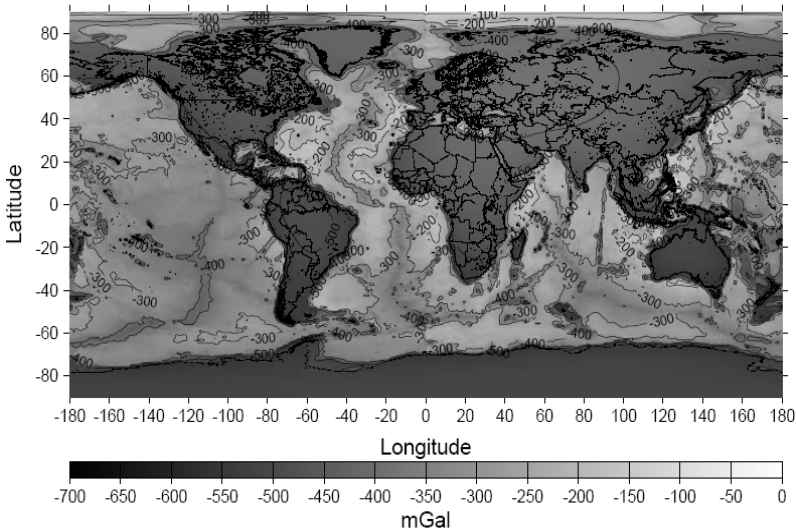
Fig. 2. The global complete bathymetric correction to the gravity anomaly at the Earth's surface computed with a spectral resolution complete to degree and order 180 of the GBM coefficients. The mean value of the ocean density contrast –1640 kg/m$^3$ was adopted.

quantities of gravity field in terms of spherical harmonics can be found for instance in *Heiskanen and Moritz (1967)*. The gravity anomalies are shown in Fig. 5; statistics see Table 4. The gravity anomalies range from –284.1 to 286.7 mGal.

The sediment, ice, and bathymetry stripped topographically corrected gravity anomalies were obtained from the gravity anomalies after adding the complete topographical correction (Fig. 1), the complete bathymetric correction (Fig. 2), the complete ice density contrast correction (Fig. 3), and the complete sediment density contrast correction (Fig. 4). Statistics of results after applying the individual corrections to the gravity anomalies are summarized in Table 4. The topographically corrected gravity anomalies range from –282.0 to 378.4 mGal (cf. Fig. 6). Comparing with the Earth's gravity anomalies, the topographically corrected gravity anomalies changed significantly especially in mountainous regions; the gravity anomalies become significantly negative after applying the complete topographical correction and revealed to a large extent a presence of the isostatic
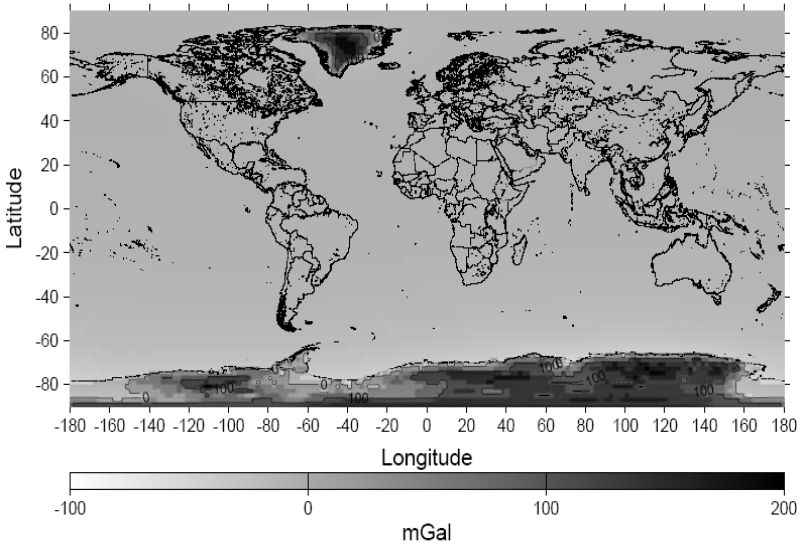
Fig. 3. The global complete ice density contrast correction to the gravity anomaly at the Earth's surface computed with a spectral resolution complete to degree and order 90 of the GITM and GEM coefficients. The mean value of the ice density contrast $-1757$ kg/m$^3$ was adopted.
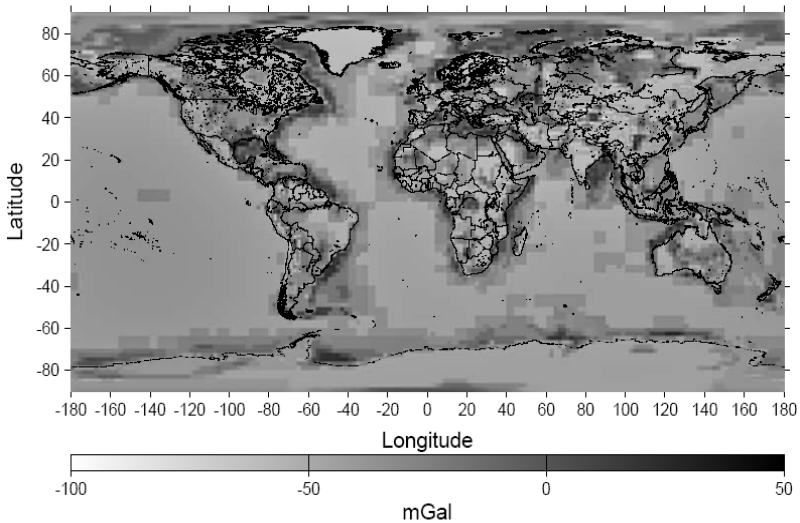


Fig. 4. The global complete sediment density contrast correction to the gravity anomaly at the Earth's surface computed with the $2 \times 2$ arc-deg spatial resolution.
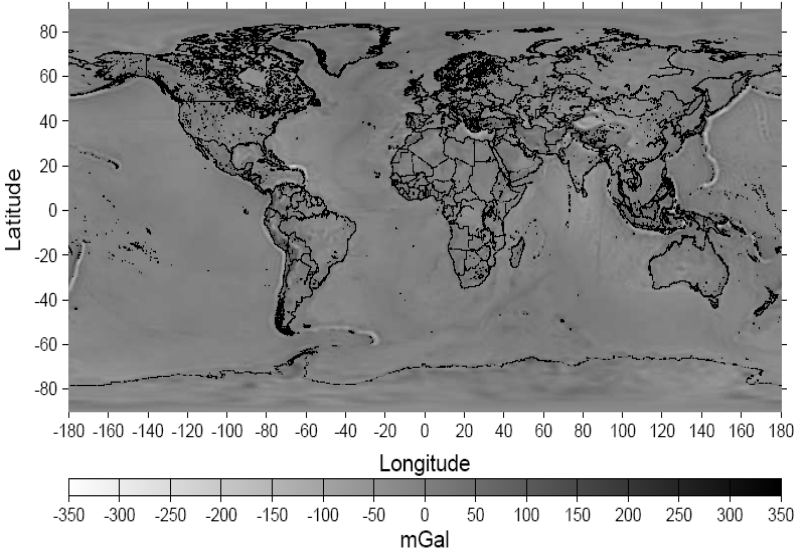
365

Fig. 5. The gravity anomalies at the Earth's surface computed with a spectral resolution complete to degree 180 of spherical harmonics.
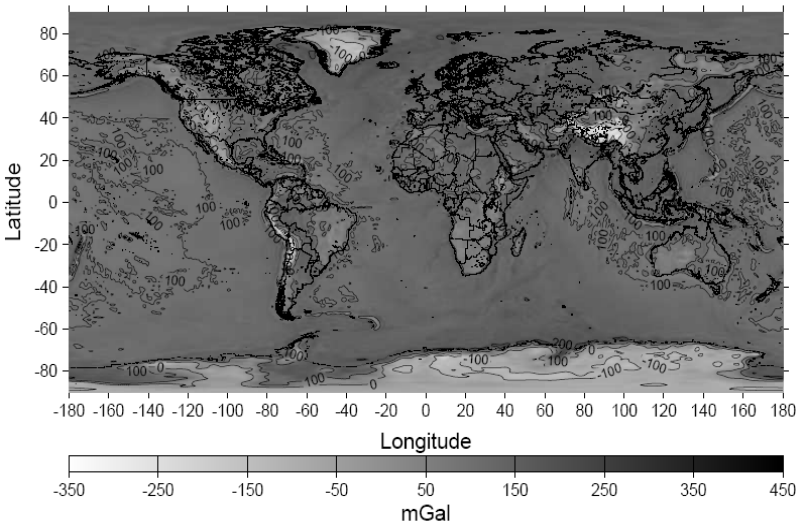


Fig. 6. The topographically corrected gravity anomalies at the Earth's surface obtained from the gravity anomalies (Fig. 5) by applying the complete topographical correction (Fig. 1).

Table 4. Statistics of the gravity anomalies, the topographically corrected gravity anomalies, the bathymetrically stripped topographically corrected gravity anomalies, and sediment, ice, and bathymetry stripped topographically corrected gravity anomalies.

| Gravity anomalies | Min [mGal] | Max [mGal] | Mean [mGal] | STD [mGal] |
|---|---|---|---|---|
| Earth's | -284.1 | 286.7 | -0.5 | 23.5 |
| Topographically corrected | -282.0 | 378.4 | 103.9 | 65.0 |
| Bathymetrically stripped topographically corrected | -749.8 | 109.5 | -271.7 | 139.2 |
| Sediment, ice, and bathymetry stripped topographically corrected | -809.6 | 81.8 | -308.3 | 121.1 |

compensation in mountainous regions. The bathymetrically stripped topographically corrected gravity anomalies range from –749.8 to 109.5 mGal (cf. Fig. 7). Since the complete bathymetric correction has mostly a long-wavelength character over continental areas, the higher-frequency spectrum of the topographically corrected gravity anomaly signal remains almost unchanged. Over the oceans, the application of the complete bathymetric correction to the topographically corrected gravity anomalies partly revealed main structures of the ocean floor relief and a global pattern of lithospheric plates more likely due to a varying density and thickness of the oceanic lithospheric plates. The sediment, ice, and bathymetry stripped topographically corrected gravity anomalies range from –796.4 to 127.4 mGal (cf. Fig. 8). Comparing with the complete topographical and bathymetric corrections, the signature of the complete ice and sediment density contrast corrections applied to the gravity anomalies is less noticeable. The complete sediment density contrast correction mainly changed the bathymetrically stripped topographically corrected gravity anomalies over areas with the largest sediment deposits in continental shelves and the Caspian Sea region. The complete ice density contrast correction significantly changed the bathymetrically stripped topographically corrected gravity anomalies in Greenland and Antarctica.

## 4. Summary and conclusions

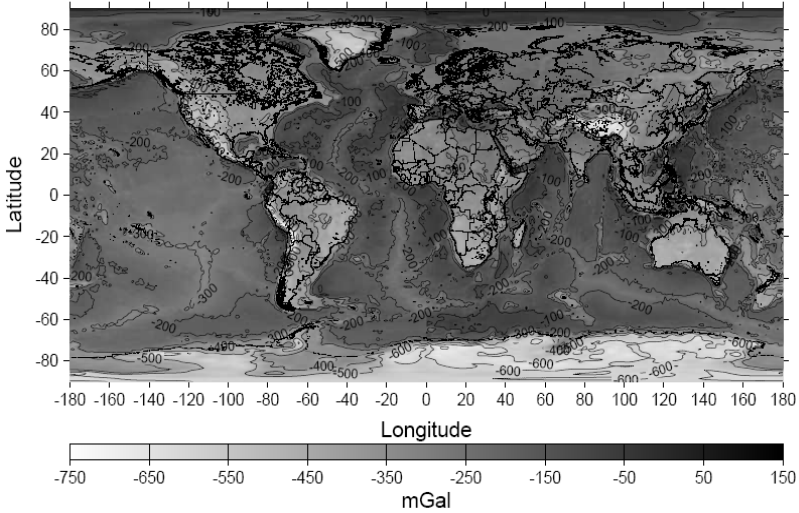We have computed and shown the complete corrections to the gravity

Fig. 7. The bathymetrically stripped topographically corrected gravity anomalies at the Earth's surface obtained from the topographically corrected gravity anomalies (Fig. 6) by applying the complete bathymetric correction (Fig. 2).
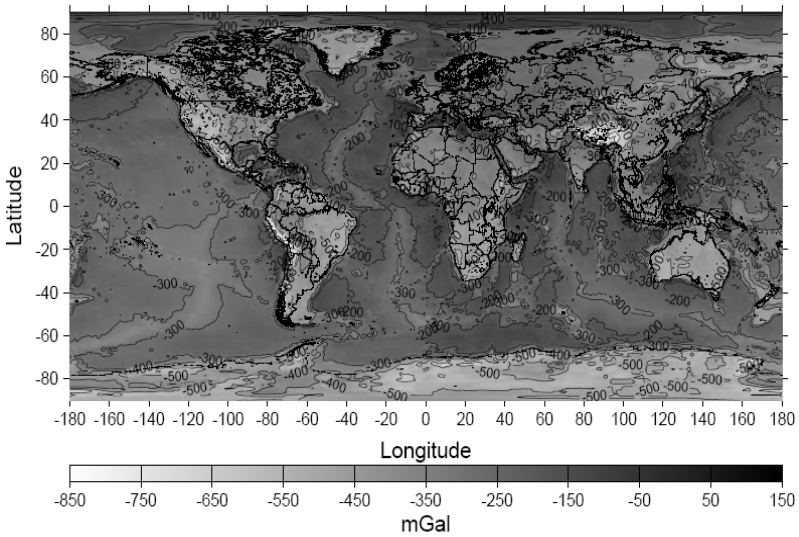


Fig. 8. The sediment, ice, and bathymetry stripped topographically corrected gravity anomalies at the Earth's surface obtained from the bathymetrically stripped topographically corrected gravity anomalies (Fig. 7) by applying the complete ice and sediment density contrast corrections (Figs. 3 and 4).

anomaly due to the topography, bathymetry, ice density contrast, and (marine and continental) sediment density contrast. The complete corrections to the gravity anomaly comprise the direct and secondary indirect effects. These corrections were further applied to the gravity anomalies in order to model the sediment, ice, and bathymetry stripped topographically corrected gravity anomalies. The topographically corrected gravity anomalies revealed a presence of the isostatic compensation in mountainous regions. The bathymetrically stripped topographically corrected gravity anomalies revealed main structures of the ocean floor relief and a global pattern of lithospheric plates more likely due to a varying density and thickness of the oceanic lithospheric plates. Comparing with the topographic and bathymetric corrections to the gravity anomalies, the ice and sediment density contrast stripping corrections are much smaller.

Large errors of modelling the complete stripping corrections to the gravity anomaly are expected especially due to errors related with uncertainties about the actual density distribution within the solid Earth's crust as well as inaccuracies of the currently available global sediment and ice thickness data. In overall, these errors can reach several dozens of miligals. The errors of the complete bathymetric correction due to the approximation of the actual ocean saltwater density by the mean value can reach a few dozens of miligals. The errors of the complete topographical correction of average crustal density are expected to be small (at the most up to a few miligals).

# References

Heiskanen W. H., Moritz H., 1967: Physical geodesy. San Francisco, W. H. Freeman and Co.

Lemoine F. G., Kenyon S. C., Factor J. K., Trimmer R. G., Pavlis N. K., Chinn D. S., Cox C. M., Klosko S. M., Luthcke S. B., Torrence M. H., Wang Y. M., Williamson R. G., Pavlis E. C., Rapp R. H., Olson T. R., 1998: The development of the joint NASA GSFC and the National Imagery and Mapping Agency (NIMA) geopotential model EGM96. NASA Tech. Publ., TP-1998-206861, NASA GSFC.

Millero F. J., Poisson A., 1981: Density of seawater and the new International Equation of State of Seawater. 1980. IMS Newsletter, Number 30, Wright (Ed.), Special Issue 1981-1982, UNESCO, Paris, France, 3 p.

Novák P., Grafarend E. W., 2006: The effect of topographical and atmospheric masses on spaceborne gravimetric and gradiometric data. Stud. Geophys. Geod., **50**, 4, 549–582; doi: 10.1007/s11200-006-0035-7macky 2.

Tenzer R., Hamayun, Vajda P., 2008: Global secondary indirect effects of topography, bathymetry, ice and sediments. Contr. Geophys. Geod., **38**, 2, 209–216.

Vajda P., Vaníček P., Meurers B., 2006: A new physical foundation for anomalous gravity. Stud. Geophys. Geod., **50**, 2, 189–216, doi:10.1007/s11200-006-0012-1.

Vajda P., Vaníček P., Novák P., Tenzer R., Ellmann A., 2007: Secondary indirect effects in gravity anomaly data inversion or interpretation. J. Geophys. Res., **112**, B06411, doi:10.1029/ 2006JB004470.

Vajda P., Ellmann A., Meurers B., Vaníček P., Novák P., Tenzer R., 2008: Global ellipsoid-referenced topographic, bathymetric and stripping corrections to gravity disturbance. Stud. Geophys. Geod., **52**, 1, 19–34, doi: 10.1007/s11200-008-0003-5.

Vaníček P., Najafi M., Martinec Z., Harrie Z., Sjöberg L. E., 1995: Higher-degree reference field in the generalised Stokes-Helmert scheme for geoid computation. J. Geod., **70**, 176–18.

Vaníček P., Tenzer R., Sjöberg L. E., Martinec Z., Featherstone W. E., 2004: New views of the spherical Bouguer gravity anomaly. Geoph. J. Int., **159**, 2, 460–472, doi:10.1111/j.1365-246X.2004.02435.x.